THE JOURNAL OF BIOLOGICAL CHEMISTRY
Vol. 279, No. 18, Issue of April 30, pp. 18146–18156, 2004
Printed in U.S.A.

The Proteolytic Processing of the Amyloid Precursor Protein Gene Family Members APLP-1 and APLP-2 Involves α-, β-, γ-, and ε-Like Cleavages

MODULATION OF APLP-1 PROCESSING BY *N*-GLYCOSYLATION*[S]

Received for publication, October 22, 2003, and in revised form, February 10, 2004
Published, JBC Papers in Press, February 17, 2004, DOI 10.1074/jbc.M311601200

Simone Eggert‡, Krzysztof Paliga§, Peter Soba, Genevieve Evin¶, Colin L. Masters¶, Andreas Weidemann, and Konrad Beyreuther

From the Zentrum für Molekulare Biologie Heidelberg, ZMBH, INF 282, 69120 Heidelberg, Germany, §Institute of Biochemistry, Medical Faculty, Christian Albrechts University Kiel, 24098 Kiel, Germany, and ¶Department of Pathology, Mental Health Research Institute, the University of Melbourne, Parkville, Victoria 3010, Australia

Amyloid precursor protein (APP) processing is of major interest in Alzheimer's disease research, since sequential cleavages by β- and γ-secretase lead to the formation of the 4-kDa amyloid Aβ protein peptide that accumulates in Alzheimer's disease brain. The processing of APP involves proteolytic conversion by different secretases leading to α-, β-, γ-, δ-, and ε-cleavages. Since modulation of these cleavages represents a rational therapeutic approach to control amyloid formation, its interference with the processing of the members of the APP gene family is of considerable importance. By using C-terminally tagged constructs of APLP-1 and APLP-2 and the untagged proteins, we have characterized their proteolytic C-terminal fragments produced in stably transfected SH-SY5Y cells. Pharmacological manipulation with specific protease inhibitors revealed that both homologues are processed by α- and γ-secretase-like cleavages, and that their intracellular domains can be released by cleavage at ε-sites. APLP-2 processing appears to be the most elaborate and to involve alternative cleavage sites. We show that APLP-1 is the only member of the APP gene family for which processing can be influenced by *N*-glycosylation. Additionally, we were able to detect p3-like fragments of APLP-1 and p3-like and Aβ-like fragments of APLP-2 in the media of stably transfected SH-SY5Y cells.

The amyloid precursor protein (APP)[1] was first identified as the precursor to Alzheimer's Aβ amyloid peptides (1). APP is a member of a multigene family comprising at least 16 orthologues (2) that encode type I integral membrane proteins with similar multidomain structures (reviewed in Ref. 2). There are two mammalian APP homologues, the APP-like proteins, termed APLP-1 (3, 4) and APLP-2 (5, 6), which share similar domain structures with APP (reviewed in Ref. 2). Transgenic mice with single knock-out of either the APP (7), APLP-1 (8), or APLP-2 (9) gene show no severe phenotype, suggesting that the mammalian APP gene family members have a redundant function. APLP-1(−/−)/APLP-2(−/−) and APP(−/−)/APLP-2 (−/−) double knock-outs are lethal, but mice with APP(−/−)/APLP-1(−/−) double knock-outs are viable (8), suggesting a physiological key role for APLP-2 during embryonic development.

The proteolytic processing of APP is central to Alzheimer's disease pathogenesis as one of the cleavage products, the 4-kDa Aβ fragment aggregates as amyloid deposits (10, 11). In the amyloidogenic pathway, APP is processed consecutively by β-secretase, which releases the Aβ N terminus, and by γ-secretase(s), which cleaves in the middle of the transmembrane domain to produce Aβ peptides ending at either Val^{40} or Ala^{42}. The β-secretase BACE (β-site APP-cleaving enzyme) was identified by four independent groups (12–15) and shown to cleave APP with the expected specificity, mainly at Met^1/Asp^1 and, to a lesser extent, at Tyr^{10}/Glu^{11} of the Aβ sequence (12). BACE cleavage releases the large ectodomain of APP (sAPPβ) and creates a membrane-anchored C-terminal fragment (CTF) of 99 amino acids. Whereas in neuronal cells APP is mostly processed by β-secretase, peripheral cells preferentially process APP in a non-amyloidogenic pathway by an alternative protease designated as α-secretase which cleaves within the Aβ domain, between Lys^{16} and Leu^{17}, and therefore precludes generation of the Aβ peptide (16, 17). α-Secretase candidates include ADAM 10 (18), ADAM 17/TACE (19, 20), and MDC-9 (21), which all belong to the family of disintegrin and metalloproteases. α-Secretase cleavage releases the APP ectodomain (sAPPα) and creates a membrane-retained C-terminal fragment of 83 amino acids (C83). The latter may be further processed by γ-secretase(s), resulting in the secretion of a small 3-kDa fragment designated p3, ending either at position 40 or 42, like the Aβ peptides. An additional cleavage within the APP ectodomain at position −12 (relative to Aβ), which was termed

* This work was supported by grants from the Deutsche Forschungsgemeinschaft project glycoproteins (to K. B.), by grants from the Deutsche Forschungsgemeinschaft through the Graduate College for Biotechnology (to K. B), grants from the Alzheimer Forschung Initiative (to A. W.), and from the Deutsche Forschungsgemeinschaft through SFB 488, the Land Baden-Württemberg, the Fond der Chemischen Industrie of Germany, the Erna-Struckmann-Foundation (to K. B.), and the National Health and Medical Research Council of Australia (to C. L. M. and G. E.). The costs of publication of this article were defrayed in part by the payment of page charges. This article must therefore be hereby marked "*advertisement*" in accordance with 18 U.S.C. Section 1734 solely to indicate this fact.

[S] The on-line version of this article (available at http://www.jbc.org) contains Fig. 1.

‡ To whom correspondence should be addressed: Zentrum für Molekulare Biologie Heidelberg, Im Neuenheimer Feld 282, D-69120 Heidelberg, Germany. Tel.: 49-6221-546846; Fax: 49-6221-545891; E-mail: s.eggert@zmbh.uni-heidelberg.de.

[1] The abbreviations used are: APP, amyloid precursor protein; APLP, amyloid precursor like protein; Aβ, amyloid Aβ protein; CTF, C-terminal fragment; AICD, APP intracellular domain; PMA, phorbol 12-myristate-13-acetate; PS, presenilin; wt, wild type; Tricine, *N*-[2-hydroxy-1,1-bis(hydroxymethyl)ethyl]glycine; DAPT, *N*-[*N*-(3,5-difluorophenacetyl-L-alanyl)]-*S*-phenylglycine *t*-butyl ester; BACE, β-site APP-cleaving enzyme.

δ-cleavage, has only been observed in hippocampal neurons so far (22). Recently, we and others have identified a presenilin-dependent cleavage at the C-terminal end of the APP transmembrane domain between Leu^{49} and Val^{50}, which we termed ϵ-cleavage (23–26), that is homologous to the S3 cleavage of Notch (27, 28). The exact mechanism of the two presenilin-dependent γ- and ϵ-cleavages within the transmembrane domain of APP remains unclear. Accumulating evidence suggests that a high molecular weight complex comprising presenilin, nicastrin (29), APH-1 (30, 31), and PEN-2 (30, 32) is responsible for γ-secretase activity. The polytopic membrane proteins PS1 and PS2 are thought to be the catalytic component of this cleavage machinery (33–36), with two critical aspartates in transmembrane domains 6 and 7 representing the catalytic site. A subset of type I membrane proteins that includes Notch, the ErbB4 tyrosine kinase receptor for neuregulins, E-cadherin, LRP, CD44, Delta, Jagged, and Nectin-1-α (37) is also processed by a presenilin-dependent, γ-secretase-like activity. For Notch, ErbB4, E-cadherin, CD44, Delta, Jagged (37), and LRP (38), it has also been demonstrated that ectodomain cleavage by a metalloprotease precedes transmembrane processing by γ-secretase-like activity. Notch S3 and APP ϵ-cleavage liberate the Notch intracellular domain and APP intracellular domain (AICD), respectively, enabling their translocation to the nucleus where they can activate transcription (39–42).

So far the processing of the APP-like proteins, APLP-1 and APLP-2, remains poorly understood. Large secretory fragments of APLP-1 (4) and APLP-2 (43) corresponding to the size of α- and β-secretase-processed secretory fragments of APP have been detected in the media of transfected cell lines. In addition, the accumulation of an APLP-1 C-terminal fragment was observed in PS-1(−/−) neurons (44). Presenilin-dependent processing of this fragment is consistent with our previous finding that PS-2 interacts with immature APLP-1 (45). To elucidate further the processing of APLP-1 and APLP-2, we developed a method to detect C-terminal fragments derived from APP, APLP-1, and APLP-2 cleavage within their transmembrane domains by stabilizing the cytosolic domains as chimeric fusion proteins with two z-domains of protein A fused in tandem (2z tag). This method previously enabled us to detect the soluble APP C-terminal fragment (ϵ-CTF or AICD) generated by proteolysis at the ϵ-site, distal to the γ-cleavage site (23). The analysis of APLP-1 and APLP-2 C-terminal fragments with the 2z tag system revealed a high similarity between the processing of APLPs and APP.

Here we show that pharmacological studies with different inhibitors of α- and γ-secretases suggest for APLP-2 the production of several α- and ϵ-like C-terminal fragments, indicating therefore that the processing of this homologue is the most complex of all three APP gene family members. Furthermore, we could detect small secreted fragments in the conditioned media of APLP-2-transfected cell lines that very likely correspond to Aβ and p3-like peptides. For APLP-1, we have identified cellular α- and ϵ-like C-terminal fragments and secreted p3-like fragments using SH-SY5Y cells stably overexpressing APLP-1. In addition, we show that cleavage of APLP-1 can be regulated by *N*-glycosylation, leading to formation of alternative p3-like fragments.

EXPERIMENTAL PROCEDURES

DNA Constructs—To generate the 2z-tagged APP derivatives, 2z-cDNA was amplified by PCR using pQE60–2z as template (23), a sense primer encoding an XhoI restriction site, and a thrombin (LVPR GS) cleavage (5′-CCCCTCGAGCTGGTTCCGCGTGGATCGAAAGAG-GAGAAATTAACC-3′) and an antisense primer encoding a stop codon and a ClaI restriction site. The resulting PCR fragment was subcloned into pBluescript SK+ (Stratagene) by using the XhoI and ClaI restriction sites. Generation of APP695–2z has been described previously (23).

To generate APLP-1-2z, the human APLP-1 cDNA cloned in pBluescript SK+ (4) was amplified by PCR with a T7 universal primer and an antisense primer that encoded a SalI restriction site just after the APLP-1 coding region (for the following 2z tag ligation). The corresponding 640-bp PCR product was digested with BamHI (coding region) and SalI (3′-end). The original cDNA (APLP-1 in pBluescript) was digested KpnI/BamHI and ligated with the PCR product in pBluescript SK+ (KpnI/SalI). The sequence of the 640-bp product was verified by sequencing. After digestion with KpnI/SalI, the full-length APLP-1 cDNA encoding the additional SalI-site at the 3′-end was ligated with the 2z-cDNA (XhoI/ClaI) into pBluescript SK+, digested with KpnI/ClaI. Subcloning of the APLP-1-2z construct in the expression vector pCEP4 cleaved with KpnI/NheI was performed by using the KpnI/XbaI sites.

To generate the APLP-2-763-2z construct, the human APLP-2-763 cDNA cloned in pBluescript SK+ was amplified by PCR with T3 reverse primer and a 3′-antisense primer encoding a SalI restriction site (for the following 2z tag ligation). The PCR product was digested with AatII (in the coding region) and SalI (3′-coding region). The original APLP-2-763 pBluescript SK+ clone was digested with BamHI/AatII, and both fragments were cloned into pBluescript SK+ (cleaved with BamHI/SalI). The XbaI/SalI fragment encoding the full-length cDNA was cloned together with 2z-cDNA (XhoI/SalI cleaved) into pCEP4 (NheI/BamHI cleaved).

APLP-1 Deletion Mutants—The human APLP-1 cDNA in pBluescript SK+ (4) was amplified by PCR using the following primer, APLP-1-2z sense primer (encoding a KpnI restriction site): D568-APLP-1-2z, 5′-GGGGGTACCCACCATGGATGAGCTGGCACCAGCTGGG-3′; R579-APLP-1-2z, 5′-GGGGGTACCCACCATGCGTGAGGCTGTATCGGCGTCTG-3′; M588-APLP-1-2z, 5′-GGGGGTACCCACCATGGGAGCGGGCGGAGGCTCCCTC-3′; M600-APLP-1-2z, 5′-GGGGGTACCCACCATGCTGCTCCTGCGCAGGAAGAAG-3′; and 3′-CGGACCTCCTTGCTGGGCAGCTGGGG-5′ for the antisense primer (encoding a SalI restriction site). The resulting PCR fragments were subcloned in pBluescript SK+, by using the KpnI and SalI restriction sites. The SalI site of the APLP-1 deletion constructs was ligated with the XhoI site of the 2z-DNA in pBluescript (XhoI/ClaI) and cloned into KpnI/ClaI-cleaved pBluescript SK+.

The human APLP-2 cDNA in pBluescript SK+ was amplified by PCR using the following primer, APLP-2 deletion mutants, APLP-2 sense primer (encoding a KpnI restriction site): M664-APLP-2-2z, 5′-CCCGGTACCACCATGATTTTCAATGCCGAGAGAG-3′; S691-APLP-2-2z, 5′-CCCGGTACCACCATGAGTAGCAGTGCTCTCATTGG-3′; M715-APLP-2-2z, 5′-CCCGGTACCACCATGCTGAGGAAGAGGCAGTATGG-3′; and 3′-GGACCTCGTCTACGTCTAAACAGCTGGGG-5′ for the antisense primer (encoding a SalI restriction site). The resulting PCR fragments were subcloned into pBluescript SK+, using the KpnI and SalI restriction sites. The SalI site of the APLP-2 deletion constructs was ligated with the XhoI site of the 2z-DNA in pBluescript (XhoI/ClaI) and cloned in the vector pBluescript SK+ KpnI/ClaI.

The template APLP-2-2z in pCEP4 was amplified by PCR using the following primer: R678-APLP-2-2z, 5′-CCCGGTACCACCATGCGGGAATCCGTGGGCCCAC-3′(encoding a KpnI restriction site); antisense primer, 3′-CCCTCCTAGGTCTAGAACTTAGCTACCG-5′. The resulting PCR fragments were subcloned in pBluescript SK+, by using the KpnI and SalI restriction sites. The SalI site of the APLP-2 deletion constructs was ligated with the XhoI site of the 2z-DNA in pBluescript (XhoI/ClaI) and cloned into the vector pBluescript SK+KpnI/ClaI.

Mutant N551Q APLP-1 was generated by site-directed mutagenesis of the human APLP-1 cDNA in pBluescript SK+ and subcloned into the vector pCEP4. Mutant R567E APLP-1 c-Myc was generated by site-directed mutagenesis of the human APLP-1 cDNA with an C-terminal Myc tag in pBluescript SK+ and subcloned into the vector pCEP4.

Antibodies—The human APLP-1-specific antiserum 150 was raised in rabbits using a synthetic peptide corresponding to residues 553–592 of human APLP-1 (46). The human APLP-2-specific antiserum 158 was raised in rabbits using the synthetic peptide sequence 672–696 of APLP-2-763, coupled to keyhole limpet hemocyanin. The APLP-1-specific antiserum 57 was raised in rabbits using keyhole limpet hemocyanin conjugates of two peptides, corresponding to human APLP-1 residues 642–650 and residues 604–614 with an additional N-terminal cysteine. An antibody recognizing the APLP-2 C terminus was purchased from Calbiochem (residues 752–763). The polyclonal antibody CT13 against the APP C terminus was raised against a synthetic peptide comprising the C-terminal 13 residues of A4CT (Eurogenetech, Brussels, Belgium) (47). The human APLP-1-specific antiserum 42464 was raised in rabbits using a synthetic peptide raised to the ectodomain of APLP-1 (residues 499–557) (4).

Cell Culture, Transfection, and Inhibitor Treatment—Human SH-SY5Y cells were cultivated and transfected with LipofectAMINE Plus (Invitrogen). For inhibitor experiments cells were treated for 7 h with Me_2SO or Me_2SO solutions of the following compounds: L-685,458, batimastat (provided by Merck, Sharp & Dohne), TAPI-2 (Peptides International), MDL28170/calpain inhibitor III (benzyloxycarbonyl-Val-Phe-CHO, carbobenzoxy-valinyl-phenylalanyl, Calbiochem), γ-secretase inhibitor IX (DAPT) (Calbiochem), MG132 (benzyloxycarbonyl-LLL-CHO, carbobenzoxy-L-leucyl-L-leucyl-L-leucinal, Calbiochem), ALLN (calpain inhibitor I, *N*-acetyl-leucyl-leucyl-norleucinal-CHO, Calbiochem), lactacystin (Calbiochem). Cells were pretreated for 1 h with tunicamycin (Sigma) or phorbol 12-myristate 13-acetate (PMA) (Calbiochem) and chased for 4 h. Control cells were treated with Me_2SO.

Immunoblotting—Lysis of cells and immunoprecipitation of APP, APLP-1, and APLP-2 was performed as described previously (48). 2z-tagged proteins were immunoprecipitated using human IgG immobilized to Sepharose (Amersham Biosciences). For the analysis of the 2z-tagged CTFs, samples were denatured in sample buffer in the absence of reducing agents and electrophoresed on 15% Tris/glycine gels. To investigate the full-length 2z-tagged proteins, samples were denatured in sample buffer with β-mercaptoethanol and separated on 8% Tris/glycine gels. After Western blotting, samples were incubated with a nonspecific rabbit antiserum as the primary antibody followed by anti-rabbit serum coupled to horseradish peroxidase and ECL detection.

Metabolic Labeling and Immunoprecipitation—Stably transfected SH-SY5Y cells cultivated in 6-cm dishes were incubated for 7 h with 200 μCi of [^{35}S]methionine/dish (Amersham Biosciences) in 1.5 ml of minimum essential medium lacking methionine (Sigma), and 5% dialyzed fetal calf serum (Sigma). The conditioned media were harvested, centrifuged at 4 °C at 10,000 × *g* for 10 min to remove cellular debris, subsequently transferred to new microcentrifuge tubes, and finally subjected to immunoprecipitation for 3 h at room temperature. The cells were washed with phosphate-buffered saline, harvested, and lysed in ice-cold lysis buffer (50 mM Tris/HCl, pH 7.5, 150 mM NaCl, 1% Nonidet P-40 (Sigma), 5 mM EDTA, 1% Triton X-100), supplemented with protease inhibitors (Complete™ protease inhibitor mixture, Roche Applied Science). The 10,000 × *g* supernatants were diluted 1:5 in buffer A (10 mM Tris/HCl, pH 7.5, 150 mM NaCl, 0.2% Nonidet P-40, 2 mM EDTA, supplemented with 0.05% SDS) and subjected to immunoprecipitation for 3 h at room temperature.

The Sepharose beads were washed three times with buffer A, twice with buffer B (10 mM Tris/HCl, pH 7.5, 500 mM NaCl, 0,2% Nonidet P-40, 2 mM EDTA), once with buffer A′ (10 mM Tris/HCl, pH 7.5, 150 mM NaCl, 0,2% Nonidet P-40, 2 mM EDTA, supplemented with 0,2% SDS), and once with buffer C (10 mM Tris/HCl, pH 7.5). The beads were resuspended in 40 μl 2× Laemmli SDS sample buffer plus β-mercaptoethanol and heated at 95 °C for 5 min. For analysis of the 2z-tagged CTFs, samples were denatured in sample buffer without β-mercaptoethanol and electrophoresed on 15% Tris/glycine gels. For analysis of the 2z-tagged full-length protein, samples were denatured in sample buffer with β-mercaptoethanol and electrophoresed on 8% Tris/glycine gels. To investigate the APLP-1 wt CTFs and the small secreted peptides, samples were denatured in sample buffer with β-mercaptoethanol and electrophoresed on 16.5% Tris/Tricine gels. The full-length protein was analyzed on 8% Tris/glycine gels.

RESULTS

Detection of the C-terminal Fragments of APP695, APLP-1, and APLP-2-763—The investigation of the C-terminal proteolytic fragments of APLP-1 and APLP-2 was performed in analogy to our previous study on APP processing (23), for which the APP cytosolic domain was stabilized as a chimeric fusion protein with a 2z tag. This tag corresponds to a tandem repeat of the z-domain of protein A that binds to the heavy chain of immunoglobulins. We have shown that the 2z tag does not alter the proteolytic processing of APP but stabilizes its C-terminal fragments and enhances their detection (23). This method has enabled the detection of a novel ε-cleavage site of APP at the C-terminal end of the transmembrane domain, between Leu^{49} and Val^{50} (23). Thus, the 2z tag was fused to the C termini of APLP-1 and APLP-2-763, and these constructs, which we termed APLP-1-2z and APLP-2-2z, respectively, were overexpressed in SH-SY5Y cells. Cell lysates from SH-SY5Y cells, stably transfected with either APP-2z, APLP-1-2z, or APLP-2-2z, were incubated with IgG-coupled Sepharose to precipitate 2z-encoding full-length proteins and C-terminal fragments (Fig. 1). Cells transfected with an empty vector were used as a control. Classification of the C-terminal fragments of APLP-1-2z and APLP-2-2z in Fig. 1 is based on pharmacological studies, and the size of these fragments is compared with deletion mutants as shown below. For APP-2z cells, two major fragments of 27 and 23 kDa were immunoprecipitated (Fig. 1*A*, *lane 1*) that represent the C-terminal cleavage products derived from APP processing at α- and ε-sites, respectively, as determined previously by N-terminal sequence analysis (23). The two upper bands at 29 and 28 kDa correspond to C-terminal fragments derived from β-secretase processing at Asp^1 and at Gln^{11}, respectively (23). The intermediate 26-kDa band represents the product of an alternative α-secretase cleavage at position Gly^{25}, as determined by N-terminal sequencing (23). For APP-2z (Fig. 1*B*, *lane 1*) the full-length protein was detected with two bands with an apparent molecular mass of 120 and 140 kDa that correspond to the immature, *N*-glycosylated form and the mature *N*- and *O*-glycosylated form, respectively (23, 48). For APLP-1-2z (Fig. 1*B*, *lane 2*), the full-length protein was detected as four bands. The three lower bands at about 90–97 kDa correspond to the immature, only *N*-glycosylated forms, whereas the upper band at about 110 kDa corresponds to the fully mature *N*- and *O*-glycosylated APLP-1 (4). The corresponding APLP-1 C-terminal fragments were detected as two doublets of 28 (α-like CTF) and 23 kDa (ε-like CTF) and a minor signal (α′-like CTF) at 27 kDa (Fig. 1*A*, *lane 3*). APLP-2 seemed to undergo a more complex processing than the other members of the APP gene family, as a subset of C-terminal fragments was detected in the range of 23–38 kDa (Fig. 1*A*,

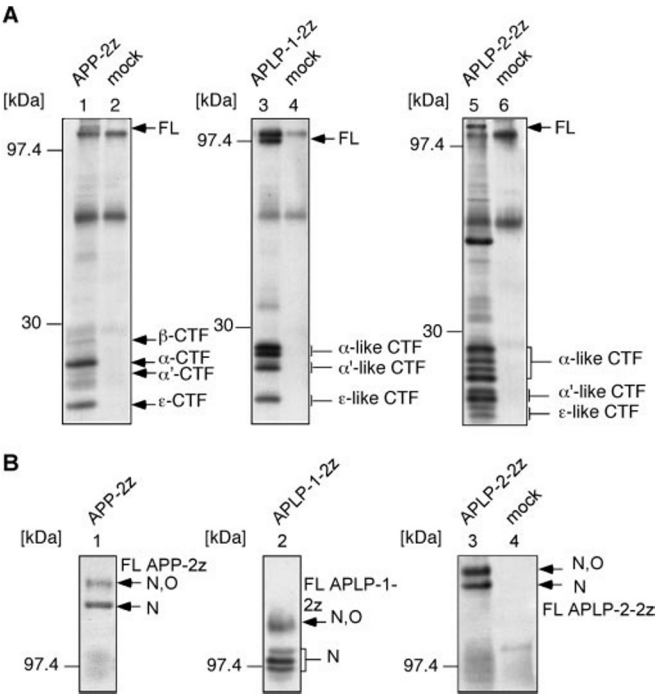

FIG. 1. **Detection of C-terminal fragments of APP695, APLP-1, and APLP-2-763.** *A*, lysates of SH-SY5Y cells stably overexpressing APP695–2z (*lane 1*), APLP-1-2z (*lane 3*), APLP-2-2z (*lane 5*) or empty vector (*lanes 2*, *4*, and *6*) were analyzed on 15% Tris/glycine gels. *FL*, full length. *B*, lysates of SH-SY5Y cells stably overexpressing APP695–2z (*lane 1*), APLP-1-2z (*lane 2*), APLP-2-2z (*lane 3*), or empty vector (*lane 4*) were analyzed on 8% Tris/glycine gels. Cell lysates were subjected to immunoprecipitation with IgG-Sepharose, followed by immunoblotting with nonspecific rabbit antiserum and ECL detection. *N*,*N*-glycosylated immature form of the full-length protein; *N*,*O*, *N*- and *O*-glycosylated mature form of the full-length protein.

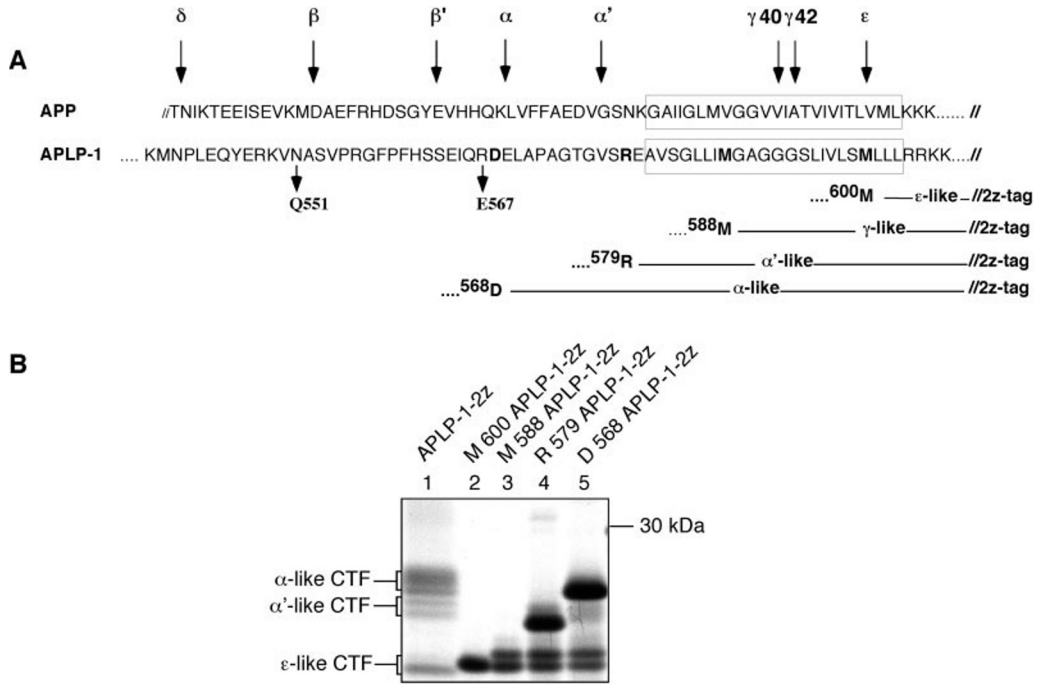

FIG. 2. **Delineating the cleavage sites of APLP-1.** *A*, comparison of the amino acid sequences of APP695 and APLP-1 of the juxtamembrane region. The sequence of APP695 shows the identified cleavage sites. Cleavage at position 25 of the Aβ sequence has been described (23). The cleavage between Leu^{49} and Val^{50} was denoted as ϵ-cleavage (23). For the sequence of APLP-1-2z the starting amino acids of the deletion mutants generated and fused to a C-terminal 2z tag (result, *B*) are indicated. The mutations at *N*-glycosylation site Asn^{551} (N551Q) and at the hypothesized α-secretase cleavage sites (R567E) that have been analyzed in Fig. 7 are also indicated. The region highlighted corresponds to the predicted transmembrane domains of APP (47) and APLP-1 (4). *B*, SH-SY5Y cells stably expressing APLP-1-2z (*B, lane 1*) were metabolically labeled for 4 h with [^{35}S]methionine followed by immunoprecipitation with IgG-Sepharose. The deletion mutants of APLP-1-2z (starting amino acids in *A*) were translated *in vitro* using rabbit reticulocyte lysates in the presence of [^{35}S]methionine and immunoprecipitated with IgG-Sepharose. (*B, lanes 2–5*) The C-terminal fragments were separated on a 15% Tris/glycine gel and visualized by autoradiography.

lane 5). The major fragments were grouped into three clusters of bands that we labeled α-like CTF, α'-like CTF, and ϵ-like CTF. For APLP-2-2z, the full-length protein was detected as two bands with an apparent molecular mass of 135 and 150 kDa that correspond to the immature, *N*-glycosylated form and the mature *N*- and *O*-glycosylated form, respectively (Fig. 1*B*, *lane 3*) (49).

Delineating the Cleavage Sites of APLP-1 and APLP-2—To narrow the cleavage sites of the C-terminal fragments derived from full-length APLP-1 and full-length APLP-2, we generated a series of deletion mutants of the APP-like proteins starting N-terminal to the transmembrane region and extending within the transmembrane domain to cover the sites, where cleavages by α-, β-, and γ-secretases are expected to occur. All deletion mutants were C-terminally fused to the 2z tag, as shown in the schematic representation (Figs. 2*A* and 3*A*). These deletion constructs were translated *in vitro* in the presence of [^{35}S]methionine and immunoprecipitated with IgG-coupled Sepharose. These samples were compared with C-terminal fragments immunoprecipitated from SH-SY5Y cells stably transfected with full-length APLP-1-2z or full-length APLP-2-2z. The deletion mutants D568-APLP-1-2z and R579-APLP-1-2z start N-terminal to the transmembrane domain of APLP-1, in the region where α-secretase cleavages are expected to occur (Fig. 2*A*) (16, 50). Comparison of the deletion mutant D568-APLP-1-2z with the cellular APLP-1-2z CTFs (Fig. 2*B, lanes 1* and *5*) indicated that the ~28-kDa APLP-1-2z CTFs resulted from cleavage around amino acid 568, about 12 residues N-terminal to the transmembrane domain, which were therefore designated as α-like CTFs. Fragments with a similar size as the deletion mutant R579-APLP-1-2z were also observed and termed α'-like CTFs (by analogy to α' cleavage of APP before Gly^{25}) (23). The deletion mutant M600-APLP-1-2z starts at the C-terminal end of the transmembrane domain of APLP-1, at a position analogous to the ϵ-cleavage site of APP (23, 24, 25, 26). The APLP-1-2z 23-kDa CTF had a similar apparent molecular weight as the *in vitro* translated M600-APLP-1-2z (Fig. 2*B*, compare *lanes 1* and *2*) and was thus named ϵ-like-CTF. We could not detect any C-terminal fragment with migration similar to the mutant Met^{588} that could represent a γ-like CTF of APLP-1-2z (Fig. 2*B*, *lanes 1* and *3*). Taken together these data indicate that APLP-1-2z is processed at cleavage sites analogous to the α- and ϵ-cleavage sites of APP.

A similar approach was used to delineate the cleavage sites of APLP-2 (Fig. 3). The deletion mutant M664-APLP-2-2z starts N-terminal to the transmembrane domain of APLP-2 in the region where β-secretase processing is expected to occur (Fig. 3*A*). Comparison of this deletion mutant (Fig. 3*B, lane 5*) with the APLP-2-2z CTFs (Fig. 3*B*, *lane 1*) shows that the minor fragments of 29 kDa could correspond to cleavage around amino acid 664 (labeled as β-like CTF). A subset of fragments with a molecular mass higher than 30 kDa (Fig. 3*A*, *lane 1*) would represent products of cleavage upstream from the β-secretase site, possibly homologous to the δ-cleavage site described for APP. The deletion mutant R678-APLP-2-2z, which begins near the expected α-cleavage site (Fig. 3*A*), migrated with a similar electrophoretic mobility as fragments of ~27 kDa produced from APLP-2-2z full-length protein (Fig. 3*B*, compare *lanes 1* and *4*); thus these were labeled α-like CTFs. The APLP-2-2z mutant that starts near the expected α'-secretase cleavage site (Fig. 3*A*) migrated similarly to minor APLP-2-2z fragments of ~25 kDa (Fig. 3*B, lane 3*), suggesting that APLP-2 also undergoes cleavage at the α'-site. The deletion mutant M715-APLP-2-2z resembles a putative fragment of APLP-2 that would be produced by cleavage at the end of the transmembrane domain, at the ϵ-site (Fig. 3*A*). This migrated

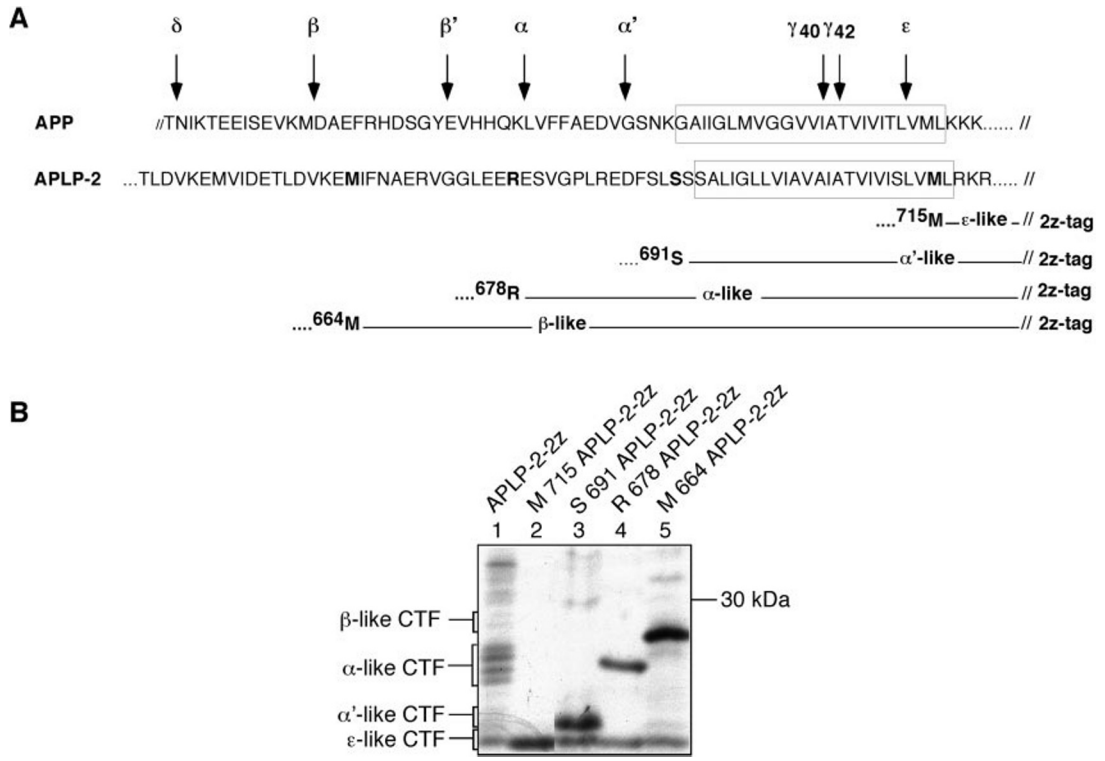

FIG. 3. **Delineating the cleavage sites of APLP-2.** *A*, comparison of the amino acid sequences of APP695 and APLP-2 of the juxtamembrane region. As for Fig. 2, the sequence of APP695 is shown with the identified cleavage sites and aligned with the sequence of APLP-2-2z and those of the generated deletion mutants. The region highlighted corresponds to the predicted transmembrane domain of APP (47) and APLP-2 (6). *B*, SH-SY5Y cells stably expressing APLP-2-2z (*B*, *lane 1*) were metabolically labeled for 4 h with [^{35}S]methionine followed by immunoprecipitation with IgG-Sepharose. The deletion mutants of APLP-2-2z (start amino acids in *A*) were translated *in vitro* using rabbit reticulocyte lysates in the presence of [^{35}S]methionine and immunoprecipitated with IgG-Sepharose. *B*, *lanes 2–5*, the C-terminal fragments were separated on a 15% Tris/glycine gel and visualized by autoradiography.

similarly to the 23-kDa APLP-2-2z CTFs, confirming that these fragments correspond to ϵ-like CTF products. Taken together, these data indicate that APLP-2-2z is processed at sites homologous to the α- and ϵ-sites and perhaps also the β- and δ-sites of APP. C-terminal fragments of APLP-2 derived from γ-cleavage in the middle of the transmembrane domain (γ-CTFs) were not expected to be observed since homologous fragments have not been detected with either APP-2z or APLP-1-2z.

The Proteolytic Processing of APP-2z, APLP-1-2z, and APLP-2-2z Is Inhibited by the Same α- and γ-Secretase Inhibitors—To characterize further the proteases involved in the proteolytic processing of APLP-1 and APLP-2, we used specific inhibitors that have been shown before to inhibit effectively the processing of APP by α- and γ-secretases, as well as several proteasome inhibitors. For inhibition of γ-secretase activity, we used the aspartyl protease inhibitor L-685,458 (35, 51), which causes an accumulation of α- and β-CTF of APP with concomitant reduction in both Aβ and ϵ-CTF (23, 25). The broad spectrum calpain inhibitor MDL28170 was tested as it is known to cause an accumulation of both α-CTF and β-CTF of APP and a concomitant decrease of APP ϵ-CTF (23, 24). Furthermore, when used at low concentration, this inhibitor can increase $A\beta_{42}$ production but has little effect on $A\beta_{40}$ production (53, 54). For inhibiting α-secretase, we employed the metalloprotease inhibitors, batimastat (55) and TAPI-2 (56–58). We also tested the effect of three different proteasome inhibitors as follows: the tripeptide aldehyde MG132 that has been reported to inhibit γ-secretase activity (28) and is also known to inhibit calpain *in vitro* (59); the calpain inhibitor I (or ALLN) that is also known to inhibit the proteasome significantly (60); and lactacystin that is a highly selective proteasome inhibitor and has no effect on aspartyl and cysteine proteases, including cathepsin D and calpain (61–63).

SH-SY5Y cells stably overexpressing APP-2z, APLP-1-2z, APLP-2-2z, and control cells were metabolically labeled for 7 h with [^{35}S]methionine in the presence of inhibitors followed by immunoprecipitation of the cell lysates with IgG-Sepharose. Treatment with the highly specific γ-secretase inhibitor L-685,458 caused an accumulation of α- and β-CTFs of APP with a concomitant decrease of the ϵ-CTF (Fig. 4*A*, *lanes 3* and *4*), as described before (23). Similarly, this inhibitor caused an accumulation of the α- and α′-like CTFs of APLP-1-2z (Fig. 4*B*, *lanes 3* and *4*) and of the α- and α′-CTFs of APLP-2-2z (Fig. 4*C*, *lanes 3* and *4*), suggesting that all these fragments are converted by γ-secretase. The formation of ϵ-like products was abolished by L-685,458 treatment, confirming that they were indeed produced by the γ-secretase complex. As described before for APP, MDL28170 caused an accumulation of α- and β-CTFs (Fig. 4*A*, *lane 5*). Similarly, the cellular concentration of α-like CTFs of APLP-1-2z and APLP-2-2z (Fig. 4, *B* and *C*, *lane 5*) was increased in the presence of this γ-secretase inhibitor. Concomitantly, the formation of APP695–2z ϵ-CTF (23), ϵ-like-CTF of APLP-1, and ϵ-like CTF of APLP-2-2z was reduced (Fig. 4, *A–C*, *lane 5*). The α-secretase inhibitors batimastat and TAPI-2 inhibited the formation APP-2z α-CTF and the generation of the α-like CTFs of APLP-1-2z and APLP-2-2z (Fig. 4, *A–C*, *lanes 6* and *7*), suggesting that these fragments were produced by an α-secretase activity. The presence of the proteasome inhibitors MG132 and lactacystin caused a strong accumulation of APP ϵ-CTF and of the ϵ-like CTFs of APLP-1 and APLP-2 (Fig. 4, *A–C*, *lanes 8* and *10*), indicating that these fragments undergo cellular degradation by the proteasome. MG132 had little effect on the levels of APP α- and β-CTFs or on the α-like fragments of APLP-1 and APLP-2 (Fig. 4, *A–C*, *lane 8*), but lactacystin treatment slightly decreased the formation of these fragments, possibly due to the regulation of the

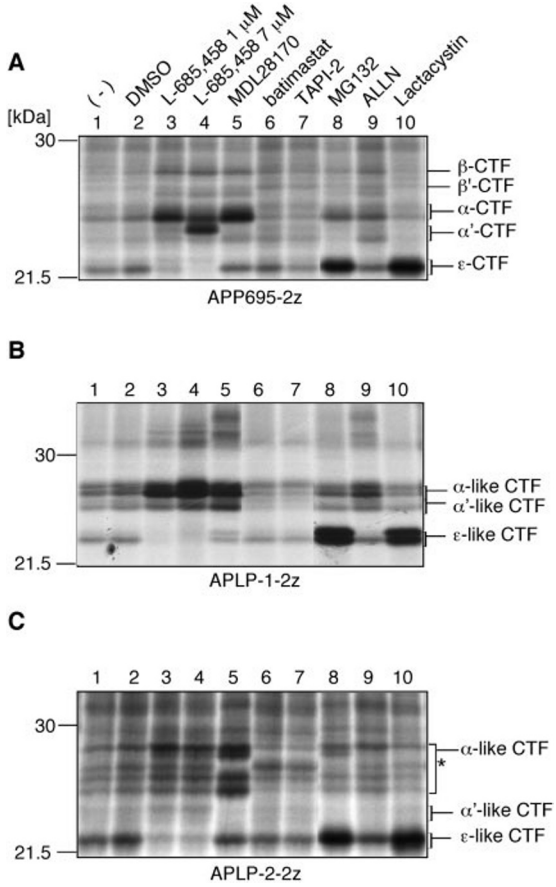

FIG. 4. **The proteolytic processing of APP-2z, APLP-1-2z, and APLP-2-2z is inhibited by the same α- and γ-secretase inhibitors.** SH-SY5Y cells stably overexpressing APP695–2z (*A*), APLP-1-2z (*B*), and APLP-2-763-2z (*C*) were metabolically labeled for 6 h with [^{35}S]methionine in the presence of the γ-secretase inhibitor L-685,458 (1 μM) (*lane 3*), L-685,458 (7 μM) (*lane 4*), the calpain inhibitor MDL28170 (100 μM) (*lane 5*), the metalloprotease inhibitors batimastat (20 μM) (*lane 6*), and TAPI-2 (40 μM) (*lane 7*), the proteasome inhibitors MG132 (20 μM) (*lane 8*), ALLN (2 μM) (*lane 9*), and lactacystin (5 μM) (*lane 10*). Untreated cells and cells incubated with Me_2SO (*DMSO*) served as a control (*lanes 1* and *2*). The cell lysates were immunoprecipitated with IgG-Sepharose, and the APP and APLP fragments were separated on a 15% Tris/glycine gel and visualized by autoradiography. (The *asterisk* indicates the APLP-2 C-terminal fragment that is reduced in the presence of a calpain-inhibitor.)

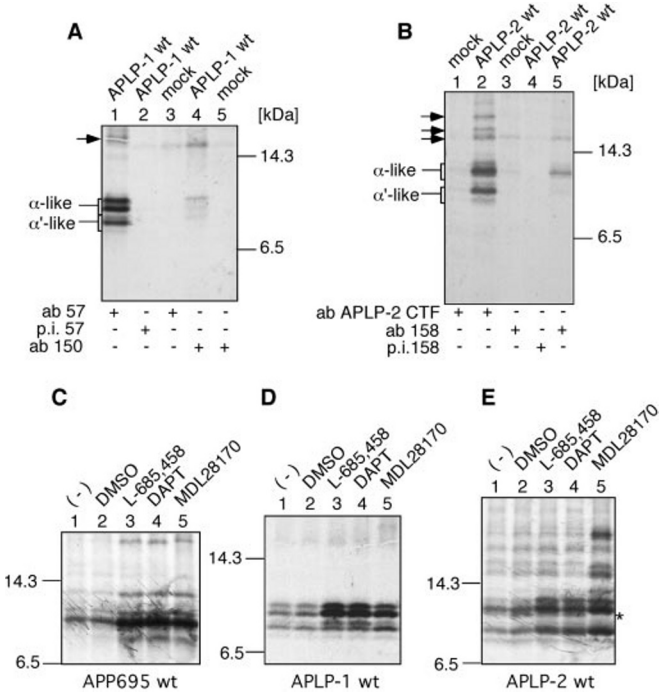

FIG. 5. **Processing of untagged APLP-1 and APLP-2.** *A*, SH-SY5Y cells stably transfected with APLP-1 or with empty vector were metabolically labeled for 4 h with [^{35}S]methionine. Cell lysates of APLP-1-transfected cells were immunoprecipitated with antibody 57 (anti-APLP-1 CTF) (*lane 1*), pre-immune (*p.i.*) serum 57 (*lane 2*), or antibody (*ab*) 150 (anti-APLP-1 Aβ-like region) (*lane 4*). Cell lysates of mock-transfected SH-SY5Y cells were immunoprecipitated with antibody 57 (*lane 3*) and antibody 150 (*lane 5*). *B*, SH-SY5Y cells stably transfected with APLP-2 or with empty vector were metabolically labeled for 4 h with [^{35}S]methionine. Cell lysates of APLP-2-transfected cells were immunoprecipitated with antibody APLP-2 CTF (*lane 2*), antibody 158 (anti-APLP-2 Aβ-like region) (*lane 5*), and pre-immune serum 158 (*lane 4*). Cell lysates of mock-transfected cells were immunoprecipitated with antibody APLP-2 CTF (*lane 1*) and antibody 158 (*lane 3*). *C*, APP695 stably transfected SH-SY5Y cells were metabolically labeled for 6 h with [^{35}S]methionine in the presence of 4 μM L-685,458 (*lane 3*), 6 μM DAPT (*lane 4*), and 100 μM MDL28170 (*lane 5*), Me_2SO (*DMSO*, *lane 2*) and compared with untreated cells (*lane 1*). Cell lysates were immunoprecipitated with antibody CT13. *D*, APLP-1-transfected SH-SY5Y cells were metabolically labeled for 6 h with [^{35}S]methionine in the presence of 4 μM L-685,458 (*lane 3*), 6 μM DAPT (*lane 4*), and 100 μM MDL28170 (*lane 5*), Me_2SO (*DMSO, lane 2*) and compared with untreated cells (*lane 1*). Cell lysates were immunoprecipitated with antibody 57. *E*, APLP-2 stably transfected SH-SY5Y cells were metabolically labeled for 6 h with [^{35}S]methionine in the presence of 4 μM L-685,458 (*lane 3*), 6 μM DAPT (*lane 4*), and 100 μM MDL28170 (*lane 5*), Me_2SO (*DMSO, lane 2*) and compared with untreated cells (*lane 1*). Cell lysates were immunoprecipitated with antibody anti-APLP-2 CTF. (The *asterisk* indicates the APLP-2 C-terminal fragment that is reduced in the presence of a calpain inhibitor.)

levels of ϵ- and ϵ-like CTFs (Fig. 4, *A–C*, *lane 10*). In contrast, the broad spectrum inhibitor ALLN caused an accumulation of APP α- and β-CTFs and α-like CTFs of APLP-1 and APLP-2. Little change was observed in the amounts of ϵ-CTF of APP and of the ϵ-like CTFs of APLP-1 and APLP-2 (Fig. 4, *A–C*, *lane 9*). ALLN also decreased the level of an uncharacterized C-terminal fragment of APLP-2 (marked by an *) with a similar effect to the other calpain inhibitor MDL28170, suggesting that this fragment may be produced by a calpain-like activity.

Processing of Untagged Wild-type APLP-1 and APLP-2—To further characterize the processing of APLP-1 and APLP-2, we produced antibodies directed to the C-terminal and Aβ-like regions of the APP homologues. These antibodies were used for immunoprecipitation of CTFs from lysates of metabolically labeled SH-SY5Y cells stably transfected with APLP-1 wt or APLP-2 wt. These antibodies did not cross-react with the other APP gene family members (data not shown). Antibody 57, directed against the C terminus of APLP-1, immunoprecipitated α-like and α′-like CTFs of 8–10 kDa which were resolved as two doublets (Fig. 5*A*, *lane 1*). This is in agreement with the previously observed pattern for the tagged constructs (Figs. 2 and 4*B*). Additionally, fragments with a size of 16 kDa were detected, analogous to the fragments of about 38 kDa of APLP-1-2z (Figs. 5, *A* and *D,* and 4*B*). Precipitation with pre-immune serum or precipitation of cell lysates of mock-transfected cells with antibody 57 failed to detect these proteins, indicating that they were specific (Fig. 5*A*, *lane 2* and *3*). Antibody 150, directed against the Aβ-like region of APLP-1, precipitated the same C-terminal fragments but with a lower affinity (Fig. 5*A*, *lane 4*).

Anti-APLP-2 C-terminal antibody (APLP-2 CTF) immunoprecipitated the C-terminal fragments of 10–12 and 15–16 kDa that would correspond to α-like, β-like CTFs, respectively (Fig. 5*B*, *lane 2*), analogous to the C-terminal fragments detected with the 2z construct (Fig. 4*C*). These fragments were not detected in mock-transfected SH-SY5Y cells (Fig. 5*B*, *lane 1*). Antibody 158, which is directed against the Aβ-like region of

APLP-2, immunoprecipitated the same fragments (Fig. 5*B*, *lane 5*) but with a weaker affinity. These fragments were not detected with the corresponding pre-immune serum (Fig. 5*B*, *lane 4*). The weak signals of fragments precipitated with antibody 158 in mock-transfected cells represent endogenous APLP-2 (Fig. 5*B*, *lane 3*). Treatment of the APP695 wt, APLP-1 wt, or APLP-2 wt transfected SH-SY5Y cells with three different γ-secretase inhibitors (L-685,458, DAPT, and MDL28170) caused the expected accumulation of APP CTFs (Fig. 5*C*, *lanes 3–5*) and of the APLP-1 (Fig. 5*D*, *lanes 3–5*) and APLP-2 CTFs (Fig. 5*E*, *lanes 3–5*), indicating that all these C-terminal fragments are further converted by γ-secretase. No C-terminal fragment of APLP-1 with a size corresponding to a β-like CTF was detectable, even in the presence of γ-secretase inhibitors (Fig. 5*D*, *lanes 1–5*). Again, APLP-2 showed the most complex processing, as found before with the 2z-tagged constructs (Fig. 4*C*).

Secretion of p3-Like Fragments from APLP-1 Transfected SH-SY5Y Cells—Since we showed processing of APLP-1 by α- and γ-secretase, we proposed to investigate if this cleavage will result in the secretion of p3-like fragments. The conditioned media of SH-SY5Y cells stably transfected with APLP-1 wt were subjected to immunoprecipitation with antibody 150 (directed to the Aβ-like region of APLP-1). The corresponding pre-immune serum and antibody 42464 (recognizing the ectodomain of APLP-1) served as controls. Antibody 150 immunoprecipitated small peptides of about 3.4 kDa from the conditioned media of stably APLP-1 transfected SH-SY5Y cells (Fig. 6*A*, *lanes 1* and *2*). Neither sAPLP-1 nor the 3.4-kDa fragments could be immunoprecipitated with the corresponding pre-immune serum (Fig. 6*A*, *lane 4*). Antibody 42464 immunoprecipitated the secreted ectodomain, sAPLP-1, but not the 3.4-kDa fragments (Fig. 6*A*, *lane 5*). The secretion of the small peptides was also reduced by treatment with the hydroxamate-based inhibitor batimastat (55) (Fig. 6*A*, *lane 3*), suggesting that they are produced by an α-secretase activity and are homologous to the p3 peptides of APP.

To characterize the proteases involved in the production of these p3-like fragments in more detail, APLP-1-transfected SH-SY5Y cells were incubated with either L-685,458, batimastat, TAPI-2, or the phorbol ester PMA, which activates protein kinase C and promotes α-secretion (18, 64, 65). The production of p3-like fragments was strongly reduced by both batimastat (Fig. 6*C*, *lane 10*) and TAPI-2 (Fig. *6C*, *lane 11*) and was increased by treatment of cells with 1 μM PMA (Fig. 6*C*, *lane 13*). These results demonstrate that APLP-1 p3-like fragments are produced by α-secretase. To demonstrate that the generation of the p3-like fragments also depends on γ-secretase, we incubated stably APLP-1-transfected SH-SY5Y cells with different concentrations of L-685,458. The γ-secretase inhibitor abolished the production of p3-like fragments of APLP-1 in a dose-dependent manner, with complete inhibition being observed at 3–7 μM inhibitor concentrations (Fig. 6*C*, *lanes 7–9*). The same results were obtained with stably APLP-1-2z-transfected SH-SY5Y cells (data not shown).

Secretion of 4.5–5-kDa Fragments from APLP-1 Is Dependent on N-Glycosylation and Is Due to the Sequential Action of α- and γ-Secretase Activities—In the experiments shown before, only α-, ε-CTFs, and p3-like fragments were detected for APLP-1-transfected cells, suggesting that APLP-1 is not converted by β-secretase. Examination of the APLP-1 sequence revealed three potential *N*-glycosylation sites at positions 331, 446, and 551 (4), the latest being positioned precisely at the site homologous to the β-secretase cleavage site of APP (Fig. 2*A* and Fig. 6*A*). Thus, we proposed that β-secretase cleavage of APLP-1 might be impeded by glycosylation of Asn^{551}. To test this hypothesis, we used tunicamycin (4, 48, 66) to block *N*-glycosylation of APLP-1. The conditioned media from APLP-1-transfected SH-SY5Y cells treated with tunicamycin were immunoprecipitated with antibody 150 (directed against the Aβ-like region), and three additional fragments with a size of about 4.5–5 kDa were observed (Fig. 7*A*, *lane 4*). We also analyzed the cell lysates of stably APP-2z, APLP-1-2z, or APLP-2-2z transfected SH-SY5Y cells after treatment with tunicamycin, thereby confirming that additionally C-terminal fragments of APLP-1 can be detected, whereas there was no difference for the production of the C-terminal fragments of APP and APLP-2 (Supplemental Material, Fig. 1). To confirm this result for APLP-1, we transfected SH-SY5Y cells with the mutant APLP-1 N551Q that bears a point mutation abolishing *N*-glycosylation at this site. Immunoprecipitation of conditioned media of APLP-1 N551Q with antibody 150 resulted in the detection of the same 4.5–5-kDa fragments (Fig. 7*A*, *lane 5*) as shown before for the tunicamycin-treated cells. We also analyzed the mutant APLP-1 R567E C-Myc that carries a point mutation at the hypothetical α-secretase cleavage site. This mutation resulted in the loss of the upper band of the p3-like

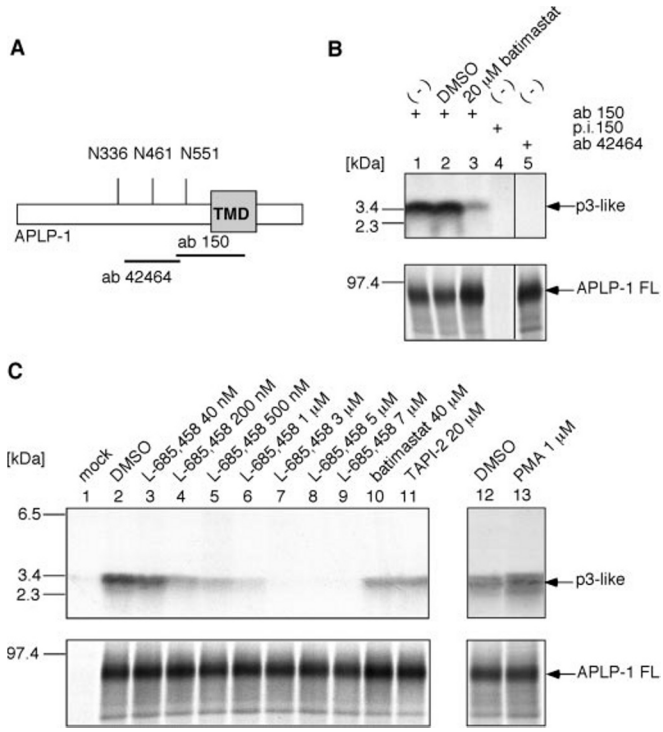

FIG. 6. **Secretion of p3-like fragments from APLP-1-transfected SH-SY5Y cells.** *A*, schematic representation of APLP-1 showing the epitopes of antibody (*ab*) 150 (Aβ-like region of APLP-1) and antibody 42464 (ectodomain of APLP-1). The three potential *N*-glycosylation sites of APLP-1 are indicated. *B*, SH-SY5Y cells stably expressing APLP-1 and control cells were metabolically labeled for 7 h with [^{35}S]methionine in the presence (*lane 3*) or absence (*lanes 1*, *2*, *4*, and *5*) of the zinc-metalloprotease inhibitor batimastat. The cell lysates and conditioned media were subjected to immunoprecipitation with antibody 150 (*lanes 1–3*). The corresponding pre-immune (*p.i.*) serum (*lane 4*) or antibody 42464 (*lane 5*) served as controls. *C*, SH-SY5Y cells stably transfected with APLP-1 wt were metabolically labeled with [^{35}S]methionine for 7 h in the presence of the following inhibitors: γ-secretase inhibitor L-685,458 at the following concentrations: 40 nM (*lane 3*), 200 nM (*lane 4*), 500 nM (*lane 5*), 1 μM (*lane 6*), 3 μM (*lane 7*), 5 μM (*lane 8*), and 7 μM (*lane 9*), and the metalloprotease inhibitors batimastat 40 μM (*lane 10*), and TAPI-2 20 μM (*lane 11*). SH-SY5Y wt cells were used as a control. SH-SY5Y cells stably transfected with APLP-1 wt were pretreated for 1 h with 1 μM PMA (*lane 13*) or Me_2SO (*DMSO*) as a control (*lane 12*) and metabolically labeled for 4 h with [^{35}S]methionine. Cell lysates and the conditioned media were immunoprecipitated with antibody 150 and separated on 8% Tris/glycine gels and 16.5% Tris/Tricine gels, respectively. *FL*, full length.

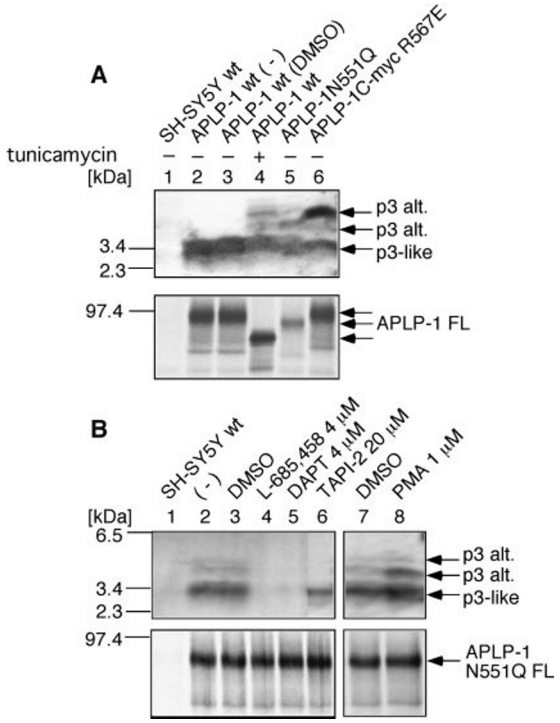

FIG. 7. **Secretion of 4.5–5-kDa fragments from APLP-1 is dependent on *N*-glycosylation and is due to the sequential action of α- and γ-secretase activities.** *A*, SH-SY5Y cells were stably transfected with APLP-1 wt (*lanes 2–4*), APLP-1 N551Q (*lane 5*), and APLP-1 R567E c-Myc (*lane 6*), metabolically labeled with [^{35}S]methionine, and compared with SH-SY5Y wt cells (*lane 1*). APLP-1 wt cells were preincubated for 1 h with tunicamycin (10 μg/ml) (*lane 4*), Me_2SO (*DMSO*, *lane 3*) or without inhibitor (*lane 2*). Conditioned media and cell lysates were immunoprecipitated with antibody 150. *FL*, full length. *B*, APLP-1 N551Q stably transfected SH-SY5Y cells were metabolically labeled with [^{35}S]methionine in the presence of the following inhibitors: 4 μM L-685,458 (*lane 4*), 4 μM DAPT (*lane 5*), 20 μM TAPI-2 (*lane 6*), Me_2SO (*DMSO*, *lane 7*), 1 μM PMA (*lane 8*). No treatment (*lane 2*) or Me_2SO (*lane 3*) were used as controls. Conditioned media and cell lysates were immunoprecipitated with antibody 150 and compared with SH-SY5Y wt cells (*lane 1*).

doublet, suggesting that part of APLP-1 becomes converted by α-secretase at position 567.

Further analysis of the corresponding cell lysates showed that total inhibition of *N*-glycosylation of APLP-1 led to a decrease in the size of full-length APLP-1 by about 10 kDa, consistent with inhibition of glycosylation at all three *N*-glycosylation sites (Fig. 7*A*, *lane 4*). The apparent molecular weight of mutant N551Q full-length protein was only slightly lower than that of APLP-1 wt since only one *N*-glycosylation site was affected (Fig. 7*A*, *lane 5*). Mutant R567E displayed a slightly lower electrophoretic mobility than APLP-1 wt due to the C-terminal Myc tag (Fig. 7*A*, *lane 6*).

To characterize further the fragments detected in the presence of tunicamycin and with the N551Q mutant from APLP-1, we treated the cells with α- and γ-secretase inhibitors. TAPI-2 clearly caused a decrease in the production of these 4.5–5-kDa fragments (Fig. 7*B*, *lane 6*), indicating they are produced by an α-secretase activity. This was further supported by showing that production of these fragments was increased after incubation of the cells with PMA, the activator of protein kinase C that enhances α-secretion (Fig. 7*B*, *lane 8*). The γ-secretase inhibitors L-685,458 (51) and DAPT (67) (Fig. 7*B*, *lanes 4* and *5*, respectively) also prevented formation of these fragments, confirming that they are produced by γ-secretase complex. Thus, our data indicate that although 4.5–5-kDa peptides can be produced from APLP-1, these are due to sequential action of α- and γ-secretase activities and do not involve β-secretase.

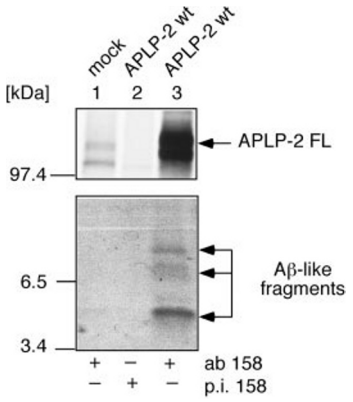

FIG. 8. **Secretion of Aβ-like fragments from APLP-2-transfected SH-SY5Y cells.** Mock-transfected SH-SY5Y cells and cells stably transfected with APLP-2 were metabolically labeled with [^{35}S]methionine. *FL*, full length. The conditioned media and cell lysates were immunoprecipitated with antibody 158 (*lanes 1* and *3*) or pre-immune serum 158 (*lane 2*).

Secretion of Aβ-like Fragments from APLP-2-transfected SH-SY5Y Cells—Multiple APLP-2 fragments corresponding to α-like and β-like CTFs were detected, which are further processed by γ-secretase (Figs. 4*C* and 5*E*). To detect p3- and possibly Aβ-like fragments, conditioned media of APLP-2 stably transfected SH-SY5Y cells were subjected to immunoprecipitation with antibody 158 that was directed against the Aβ-like region of APLP-2. Secretory peptides with a size of 4.5–8 kDa were detected that may represent products from β- and δ-cleavage, further processed by γ-secretase (Fig. 8, *lane 3*). The pre-immune serum failed to detect these fragments (Fig. 8, *lane 2*) that were also absent from antibody 158 immunoprecipitates from media of mock-transfected cells (Fig. 8, *lane 1*). Since the only methionine present in the Aβ region of APLP-2 is near the predicted β-secretase site (residue 664; Fig. 3*A*), only fragments resulting from cleavage upstream from Met^{664} are detectable in the immunoprecipitates by autoradiography. Thus, our results suggest that APLP-2 can generate Aβ-like products. Whether these are due to the action of an α-secretase or a β-secretase activity remains to be clarified.

DISCUSSION

The proteolytic processing of the mammalian APP gene family members APLP-1 and APLP-2 has been poorly investigated so far, although further characterization of the metabolism of the APP-related proteins is of interest for evaluating therapeutic strategies that target APP processing. The use of C-terminally 2z-tagged APLP-1 and APLP-2 chimeric constructs enabled us to detect several C-terminal fragments with a size expected for products from cleavages N-terminal to the transmembrane domain and within the transmembrane domain, as expected for a conversion by α-, β-, and γ-secretases (Fig. 1). Studies with various cell lines have demonstrated that the principal cleavage of APP occurs after Lys^{16} within the Aβ domain and is due to α-secretase activity (16, 17), but multiple minor cleavages around this site have also been reported (22, 23, 68). It has been shown previously (50, 68–71) that various point mutations near the α-cleavage site of APP, at Lys^{16} or at the adjacent amino acids, or deletions in this region have little or no effect on the secretion of the APP ectodomain. So the principal determinants of APP cleavage by α-secretase appear to be the distance of the hydrolyzed bond from the membrane (12 or 13 residues) and a helical conformation (50). Pharmacological studies have shown that α-secretase is a zinc-dependent metalloprotease, and that its activity can be blocked by peptide hydroxamates (72).

We were able to show that APLP-1 and APLP-2 are processed by an α-secretase activity similarly to APP. For both homologues, we detected several C-terminal fragments with a size similar to α-CTF of APP (Figs. 1 and 5). Moreover, comparison with *in vitro* translated deletion mutants starting N-terminal to their transmembrane domains revealed that the main cleavages occurred at about 12 amino acids N-terminal to the transmembrane domains (Figs. 3 and 4) at sites homologous to the APP α-cleavage site. Like for APP, these α-secretase products were the predominant C-terminal fragments produced during normal cellular metabolism. The heterogeneity of these fragments may be due to the fact that α-secretase activity is exerted by several proteases (TACE/ADAM 17, ADAM 10, and MDC9), which are able to cleave APP and might also process APLP-1 and APLP-2. That the metalloprotease inhibitors batimastat and TAPI-2 also reduced the levels of APLP-1 and APLP-2 α-like C-terminal fragments in a similar manner as for APP confirms that these fragments are generated by an α-secretase activity. In contrast to APLP-2, we found no evidence for β-secretase cleavage of APLP-1. This was deduced from the size of the C-terminal fragments detected (Figs. 2 and 3). Even in the presence of γ-secretase inhibitors that lead to an accumulation of α- and β-C-terminal fragments of APP, no accumulation of an APLP-1 fragment with a size expected for a β-secretase cleavage product was observed. In contrast, several fragments of APLP-2 were observed that have a size similar to the deletion mutant M664-APLP-2-2z, which mimics β-cleaved APLP-2. It is known that BACE can cleave a sequence between *X/Y* with *X* = Phe, Tyr, Met, or Leu and *Y* = Met, Ala, Ser, Gln, Glu, or Asp (73). The sequence of APLP-2 in the region of Met^{664} shows a leucine and an aspartate at positions 659 and 660, respectively, that could be potential BACE-cleavage sites. Unlike α- and γ-secretase, the aspartyl protease BACE that generates the N terminus of Aβ shows a higher substrate specificity (73, 74). So far the only reported BACE substrates besides APP are the α2,6-sialyltransferase and the cell adhesion protein P-selectin glycoprotein ligand-1 (75–77). BACE cleaves APP at two sites, mainly before Asp^{1} and to a lesser extent before Glu^{11} of Aβ. Additionally, minor forms of Aβ peptides starting at Val^{3} and Ile^{6} have been identified (78) that may result from cleavages by alternative proteases (12). Furthermore, additional cleavage sites were also detected in certain systems that appear to be cell-specific, *e.g.* δ-cleavage of APP695 at position −12 (Aβ numbering) in hippocampal neurons (22). The enzymatic activity that carries out δ-cleavage remains to be characterized. C-terminal fragments of APLP-1 and APLP-2 with a molecular weight higher than the α-like fragments (30 and 38 kDa) were observed that might be generated by a similar enzyme activity.

The C-terminal fragments of APP, generated by α- and β-secretase activities, are subsequently cleaved within the transmembrane domain by γ-secretase, resulting in the release of small peptides termed p3 and Aβ, respectively, and of the APP intracellular domain, AICD. γ-Secretase appears to be a multiprotein complex comprising the proteins APH-1, nicastrin, PEN-2, and presenilin (30). γ-Secretase cleaves APP with a loose sequence specificity in the middle of the transmembrane region (47, 79–83), as well as near the membrane/cytosol interface (23–26). The exact mechanism of γ-secretase cleavage is still unclear, although a recent study shows that a signal peptide peptidase with a membrane topology and consensus motifs homologous to presenilin (84) is also capable to process signal peptides at alternative membrane sites. A novel concept is emerging that suggests that transmembrane domains can be processed within a hydrophobic phospholipid environment and several other classes of polytopic membrane proteases have now been identified that include the putative metalloprotease S2P that effects site 2 cleavage of the sterol-regulatory element binding protein (85) and the rhomboid family of serine proteases (86, 87).

A whole collection of γ-secretase substrates has now been found that includes Notch, the ErbB4 tyrosine kinase receptor for neuregulins, E-cadherin, LRP, CD44, Delta, Jagged, and Nectin-1-α (37). For all these proteins, it has also been demonstrated that ectodomain cleavage by a metalloprotease precedes transmembrane processing by a γ-secretase-like activity. A dual γ-secretase cleavage has so far been demonstrated only for APP, Notch, and CD44 and in this report for APLP-1 and APLP-2. The exact relationship between these two cleavages has not been fully elucidated yet, although it has been reported recently (88) that increased production of γ^{42}-CTF of APP by mutant presenilins or mutant APP also increases the production of a CTF starting at position 49, near the ϵ-cleavage site (position 50). We were able to detect ϵ-like C-terminal fragments of APLP-1 and APLP-2 that are generated by γ-secretase activity using 2z-tagged constructs. Comparison of cellular fragments with *in vitro* translated standards indicates that these correspond to cleavages at sites homologous to ϵ-cleavage of APP and S3 cleavage of Notch. Furthermore, the γ-secretase inhibitors L-685,458 and MDL28170 decreased the production of these fragments significantly with a concomitant accumulation of α-like C-terminal fragments of APLP-1 and α-, β-, and δ-like C-terminal fragments of APLP-2 (Fig. 4). This result was confirmed by showing that three different γ-secretase inhibitors caused a significant accumulation of α-like C-terminal fragments of untagged APLP-1 and α-, β-, and δ-like fragments of untagged APLP-2 (Fig. 5). Fragments resulting from ϵ-like cleavages at the C-terminal end of the transmembrane domain of APLP-1 and APLP-2 have been identified by Gu *et al.* (24) in rodent brain with matrix-assisted laser desorption ionization/time of flight analysis, starting at position 716 of rat APLP-2 and at positions 605, 604, and 602 of mouse APLP-1. Therefore, APLP-1 and APLP-2 represent two further substrates of γ-secretase. As for APP, substrate activation requires cleavages by metalloproteases that result in shedding of the large ectodomain, enabling cleavage by γ-secretase within the transmembrane domain and release of the intracellular domain. The finding that APP homologues can be processed to release intracellular domains is consistent with a signaling function similar to that of APP. There is a high degree of conservation within the cytosolic domains of the APP gene family members, and Scheinfeld *et al.* (89) and Walsh *et al.* (46) reported that all three proteins can be stabilized by Fe65 and translocate to the nucleus. These two groups also described the existence of C-terminal fragments of APLP-1 and APLP-2 that can be modulated by γ-secretase inhibitors (46, 89).

The finding of α- and γ-C-terminal fragments of APLP-1 prompted us to investigate the possible production of p3-like fragments. We were able to detect a secreted p3-like fragment of APLP-1 generated during normal cellular metabolism (Fig. 6). The γ-secretase inhibitor L-685,458 as well as the metalloprotease inhibitors TAPI-2 and batimastat decreased the production of this fragment significantly, whereas the phorbol ester PMA increased its detection, strongly suggesting that it was generated by α- and γ-secretase activities (Fig. 6). The finding that R567E APLP-1 C-Myc, a mutant that carries a point mutation at the potential α-secretase cleavage site, does not produce the upper band of the secreted p3-like doublet, further supports that some processing of APLP-1 occurs at position 567, as shown by delineating the cleavage sites that produce the α-like C-terminal fragments (Figs. 2 and 7).

APLP-1 is a highly glycosylated protein with three potential

N-glycosylation sites at positions Asn^{336}, Asn^{461}, and Asn^{551}. *N*-Glycosylation site Asn^{551} is positioned exactly at the site homologous to the APP β-secretase cleavage site. We were able to show that inhibition of *N*-glycosylation by introducing a point mutation at site 551 resulted in the generation of alternative secreted fragments of 4.5–5 kDa. Treatment of cells with the *N*-glycosylation inhibitor tunicamycin caused a similar effect. The metalloprotease inhibitors batimastat and TAPI-2 and the γ-secretase inhibitors L-685,458 and DAPT also decreased the production of the alternative p4.5–5 fragments, although these were increased in the presence of PMA (Fig. 7). This suggests that these fragments are also generated by an α- and γ-secretase activity and not by BACE (Fig. 7). Our data indicate that the processing of APLP-1 can be influenced via *N*-glycosylation, thereby regulating metalloprotease cleavages that seem to be dependent on a certain helical conformation N-terminal to the transmembrane domain of APLP-1. Similarly, it has been reported recently that *O*-glycosylation can modulate proteolytic processing of the low density lipoprotein receptor-related protein 1 (LRP1) and the apolipoprotein E (apoE) receptor-2 (apoER2) (90). Since APLP-1 cleavage is also modulated by glycosylation, this result offers the intriguing possibility that glycosylation might represent a general mechanism of regulation of proteolysis. Whether *O*-glycosylation of the APP gene family members influences their proteolytic conversion remains to be clarified.

We have also been able to detect small, secreted fragments of APLP-2 in stably transfected SH-SY5Y cells. Their size corresponds to that of an Aβ-like fragment, but the enzyme activities that are responsible for their generation will have to be investigated in more detail.

Taken together, our results indicate that APLP-1 and APLP-2 are processed by α-, γ-, and ϵ-cleavages in a similar manner as APP. APLP-2 undergoes a processing more extensive and more similar to that of APP, also including β-like cleavages. This might be expected, since APP and APLP-2 are evolutionarily more closely related to each other than to APLP-1, which represents the ancestral form of the APP gene family members (2). Our findings suggest that despite some differences in the processing of the members of the APP gene family, future treatment of patients with Alzheimer's disease by modulation of APP processing should take into consideration the effect on APLP-1 and APLP-2 processing. Whereas all three proteins are γ-secretase substrates and show their processing to be influenced by γ-secretase inhibitors, we have no evidence so far that APLP-1 is a substrate of BACE. However, since the ubiquitously expressed APLP-2 might be cleaved by BACE, future work will reveal the impact of BACE inhibition on neuronal survival and plasticity and on therapeutic approaches directed against APP processing that might interfere with APLP2 processing as well.

Acknowledgments—We thank Dr. Mark Shearman, Dr. Dirk Beher, and the Medicinal Chemistry Department at Merck, Sharp & Dohne for generously providing L-685.458, batimastat, and several γ-secretase inhibitors before publication; Dr. Dirk Görlich for a 2z-cDNA encoding plasmid; Dr. Stefan Kins for critical reading of the manuscript; Dr. Gerd Multhaup for the APLP-1 antibody 42464; and Dr. Tobias Hartmann for the APP antibody CT13.

REFERENCES

1. Kang, J., Lemaire, H. G., Unterbeck, A., Salbaum, J. M., Masters, C. L., Grzeschik, K. H., Multhaup, G., Beyreuther, K., and Muller-Hill, B. (1987) *Nature* **325,** 733–736
2. Coulson, E. J., Paliga, K., Beyreuther, K., and Masters, C. L. (2000) *Neurochem. Int.* **36,** 175–184
3. Wasco, W., Bupp, K., Magendantz, M., Gusella, J. F., Tanzi, R. E., and Solomon, F. (1992) *Proc. Natl. Acad. Sci. U. S. A.* **89,** 10758–10762
4. Paliga, K., Peraus, G., Kreger, S., Durrwang, U., Hesse, L., Multhaup, G., Masters, C. L., Beyreuther, K., and Weidemann, A. (1997) *Eur. J. Biochem.* **250,** 354–363
5. Wasco, W., Gurubhagavatula, S., Paradis, M. D., Romano, D. M., Sisodia, S. S., Hyman, B. T., Neve, R. L., and Tanzi, R. E. (1993) *Nat. Genet.* **5,** 95–100
6. Slunt, H. H., Thinakaran, G., Von Koch, C., Lo, A. C., Tanzi, R. E., and Sisodia, S. S. (1994) *J. Biol. Chem.* **269,** 2637–2644
7. Zheng, H., Jiang, M., Trumbauer, M. E., Sirinathsinghji, D. J., Hopkins, R., Smith, D. W., Heavens, R. P., Dawson, G. R., Boyce, S., Conner, M. W., and *et al.* (1995) *Cell* **81,** 525–531
8. Heber, S., Herms, J., Gajic, V., Hainfellner, J., Aguzzi, A., Rulicke, T., von Kretzschmar, H., von Koch, C., Sisodia, S., Tremml, P., Lipp, H. P., Wolfer, D. P., and Muller, U. (2000) *J. Neurosci.* **20,** 7951–7963
9. von Koch, C. S., Zheng, H., Chen, H., Trumbauer, M., Thinakaran, G., van der Ploeg, L. H., Price, D. L., and Sisodia, S. S. (1997) *Neurobiol. Aging* **18,** 661–669
10. Glenner, G. G., and Wong, C. W. (1984) *Biochem. Biophys. Res. Commun.* **120,** 885–890
11. Masters, C. L., Multhaup, G., Simms, G., Pottgiesser, J., Martins, R. N., and Beyreuther, K. (1985) *EMBO J.* **4,** 2757–2763
12. Vassar, R., Bennett, B. D., Babu-Khan, S., Kahn, S., Mendiaz, E. A., Denis, P., Teplow, D. B., Ross, S., Amarante, P., Loeloff, R., Luo, Y., Fisher, S., Fuller, J., Edenson, S., Lile, J., Jarosinski, M. A., Biere, A. L., Curran, E., Burgess, T., Louis, J. C., Collins, F., Treanor, J., Rogers, G., and Citron, M. (1999) *Science* **286,** 735–741
13. Yan, R., Bienkowski, M. J., Shuck, M. E., Miao, H., Tory, M. C., Pauley, A. M., Brashier, J. R., Stratman, N. C., Mathews, W. R., Buhl, A. E., Carter, D. B., Tomasselli, A. G., Parodi, L. A., Heinrikson, R. L., and Gurney, M. E. (1999) *Nature* **402,** 533–537
14. Sinha, S., Anderson, J. P., Barbour, R., Basi, G. S., Caccavello, R., Davis, D., Doan, M., Dovey, H. F., Frigon, N., Hong, J., Jacobson-Croak, K., Jewett, N., Keim, P., Knops, J., Lieberburg, I., Power, M., Tan, H., Tatsuno, G., Tung, J., Schenk, D., Seubert, P., Suomensaari, S. M., Wang, S., Walker, D., John, V., and *et al.* (1999) *Nature* **402,** 537–540
15. Hussain, I., Powell, D. J., Howlett, D. R., Chapman, G. A., Gilmour, L., Murdock, P. R., Tew, D. G., Meek, T. D., Chapman, C., Schneider, K., Ratcliffe, S. J., Tattersall, D., Testa, T. T., Southan, C., Ryan, D. M., Simmons, D. L., Walsh, F. S., Dingwall, C., and Christie, G. (2000) *Mol. Cell. Neurosci.* **16,** 609–619
16. Esch, F. S., Keim, P. S., Beattie, E. C., Blacher, R. W., Culwell, A. R., Oltersdorf, T., McClure, D., and Ward, P. J. (1990) *Science* **248,** 1122–1124
17. Wang, R., Meschia, J. F., Cotter, R. J., and Sisodia, S. S. (1991) *J. Biol. Chem.* **266,** 16960–16964
18. Lammich, S., Kojro, E., Postina, R., Gilbert, S., Pfeiffer, R., Jasionowski, M., Haass, C., and Fahrenholz, F. (1999) *Proc. Natl. Acad. Sci. U. S. A.* **96,** 3922–3927
19. Buxbaum, J. D., Liu, K. N., Luo, Y., Slack, J. L., Stocking, K. L., Peschon, J. J., Johnson, R. S., Castner, B. J., Cerretti, D. P., and Black, R. A. (1998) *J. Biol. Chem.* **273,** 27765–27767
20. Slack, B. E., Ma, L. K., and Seah, C. C. (2001) *Biochem. J.* **357,** 787–794
21. Koike, H., Tomioka, S., Sorimachi, H., Saido, T. C., Maruyama, K., Okuyama, A., Fujisawa-Sehara, A., Ohno, S., Suzuki, K., and Ishiura, S. (1999) *Biochem. J.* **343,** 371–375
22. Simons, M., de Strooper, B., Multhaup, G., Tienari, P. J., Dotti, C. G., and Beyreuther, K. (1996) *J. Neurosci.* **16,** 899–908
23. Weidemann, A., Eggert, S., Reinhard, F. B., Vogel, M., Paliga, K., Baier, G., Masters, C. L., Beyreuther, K., and Evin, G. (2002) *Biochemistry* **41,** 2825–2835
24. Gu, Y., Misonou, H., Sato, T., Dohmae, N., Takio, K., and Ihara, Y. (2001) *J. Biol. Chem.* **276,** 35235–35238
25. Sastre, M., Steiner, H., Fuchs, K., Capell, A., Multhaup, G., Condron, M. M., Teplow, D. B., and Haass, C. (2001) *EMBO Rep* **2,** 835–841
26. Yu, C., Kim, S. H., Ikeuchi, T., Xu, H., Gasparini, L., Wang, R., and Sisodia, S. S. (2001) *J. Biol. Chem.* **276,** 43756–43760
27. Schroeter, E. H., Kisslinger, J. A., and Kopan, R. (1998) *Nature* **393,** 382–386
28. De Strooper, B., Annaert, W., Cupers, P., Saftig, P., Craessaerts, K., Mumm, J. S., Schroeter, E. H., Schrijvers, V., Wolfe, M. S., Ray, W. J., Goate, A., and Kopan, R. (1999) *Nature* **398,** 518–522
29. Yu, G., Nishimura, M., Arawaka, S., Levitan, D., Zhang, L., Tandon, A., Song, Y. Q., Rogaeva, E., Chen, F., Kawarai, T., Supala, A., Levesque, L., Yu, H., Yang, D. S., Holmes, E., Milman, P., Liang, Y., Zhang, D. M., Xu, D. H., Sato, C., Rogaev, E., Smith, M., Janus, C., Zhang, Y., Aebersold, R., Farrer, L. S., Sorbi, S., Bruni, A., Fraser, P., and St. George-Hyslop, P. (2000) *Nature* **407,** 48–54
30. Francis, R., McGrath, G., Zhang, J., Ruddy, D. A., Sym, M., Apfeld, J., Nicoll, M., Maxwell, M., Hai, B., Ellis, M. C., Parks, A. L., Xu, W., Li, J., Gurney, M., Myers, R. L., Himes, C. S., Hiebsch, R., Ruble, C., Nye, J. S., and Curtis, D. (2002) *Dev. Cell* **3,** 85–97
31. Goutte, C., Tsunozaki, M., Hale, V. A., and Priess, J. R. (2002) *Proc. Natl. Acad. Sci. U. S. A.* **99,** 775–779
32. Steiner, H., Winkler, E., Edbauer, D., Prokop, S., Basset, G., Yamasaki, A., Kostka, M., and Haass, C. (2002) *J. Biol. Chem.* **277,** 39062–39065
33. Wolfe, M. S., Xia, W., Ostaszewski, B. L., Diehl, T. S., Kimberly, W. T., and Selkoe, D. J. (1999) *Nature* **398,** 513–517
34. De Strooper, B., Saftig, P., Craessaerts, K., Vanderstichele, H., Guhde, G., Annaert, W., Von Figura, K., and Van Leuven, F. (1998) *Nature* **391,** 387–390
35. Li, Y. M., Xu, M., Lai, M. T., Huang, Q., Castro, J. L., DiMuzio-Mower, J., Harrison, T., Lellis, C., Nadin, A., Neduvelil, J. G., Register, R. B., Sardana, M. K., Shearman, M. S., Smith, A. L., Shi, X. P., Yin, K. C., Shafer, J. A., and Gardell, S. J. (2000) *Nature* **405,** 689–694
36. Kimberly, W. T., Xia, W., Rahmati, T., Wolfe, M. S., and Selkoe, D. J. (2000) *J. Biol. Chem.* **275,** 3173–3178
37. De Strooper, B. (2003) *Neuron* **38,** 9–12
38. Quinn, K. A., Pye, V. J., Dai, Y. P., Chesterman, C. N., and Owensby, D. A. (1999) *Exp. Cell Res.* **251,** 433–441
39. Jarriault, S., Brou, C., Logeat, F., Schroeter, E. H., Kopan, R., and Israel, A.

(1995) *Nature* **377,** 355–358
40. Lu, F. M., and Lux, S. E. (1996) *Proc. Natl. Acad. Sci. U. S. A.* **93,** 5663–5667
41. Cao, X., and Sudhof, T. C. (2001) *Science* **293,** 115–120
42. Minopoli, G., de Candia, P., Bonetti, A., Faraonio, R., Zambrano, N., and Russo, T. (2001) *J. Biol. Chem.* **276,** 6545–6550
43. Webster, M. T., Groome, N., Francis, P. T., Pearce, B. R., Sherriff, F. E., Thinakaran, G., Felsenstein, K. M., Wasco, W., Tanzi, R. E., and Bowen, D. M. (1995) *Biochem. J.* **310,** 95–99
44. Naruse, S., Thinakaran, G., Luo, J. J., Kusiak, J. W., Tomita, T., Iwatsubo, T., Qian, X., Ginty, D. D., Price, D. L., Borchelt, D. R., Wong, P. C., and Sisodia, S. S. (1998) *Neuron* **21,** 1213–1221
45. Weidemann, A., Paliga, K., Durrwang, U., Czech, C., Evin, G., Masters, C. L., and Beyreuther, K. (1997) *Nat. Med.* **3,** 328–332
46. Walsh, D. M., Fadeeva, J. V., LaVoie, M. J., Paliga, K., Eggert, S., Kimberly, W. T., Wasco, W., and Selkoe, D. J. (2003) *Biochemistry* **42,** 6664–6673
47. Grziwa, B., Grimm, M. O., Masters, C. L., Beyreuther, K., Hartmann, T., and Lichtenthaler, S. F. (2003) *J. Biol. Chem.* **278,** 6803–6808
48. Weidemann, A., Konig, G., Bunke, D., Fischer, P., Salbaum, J. M., Masters, C. L., and Beyreuther, K. (1989) *Cell* **57,** 115–126
49. Lyckman, A. W., Confaloni, A. M., Thinakaran, G., Sisodia, S. S., and Moya, K. L. (1998) *J. Biol. Chem.* **273,** 11100–11106
50. Sisodia, S. S. (1992) *Proc. Natl. Acad. Sci. U. S. A.* **89,** 6075–6079
51. Shearman, M. S., Beher, D., Clarke, E. E., Lewis, H. D., Harrison, T., Hunt, P., Nadin, A., Smith, A. L., Stevenson, G., and Castro, J. L. (2000) *Biochemistry* **39,** 8698–8704
52. Higaki, J., Quon, D., Zhong, Z., and Cordell, B. (1995) *Neuron* **14,** 651–659
53. Mathews, P. M., Jiang, Y., Schmidt, S. D., Grbovic, O. M., Mercken, M., and Nixon, R. A. (2002) *J. Biol. Chem.* **277,** 36415–36424
54. Citron, M., Diehl, T. S., Gordon, G., Biere, A. L., Seubert, P., and Selkoe, D. J. (1996) *Proc. Natl. Acad. Sci. U. S. A.* **93,** 13170–13175
55. Parvathy, S., Hussain, I., Karran, E. H., Turner, A. J., and Hooper, N. M. (1998) *Biochemistry* **37,** 1680–1685
56. Arribas, J., Coodly, L., Vollmer, P., Kishimoto, T. K., Rose-John, S., and Massague, J. (1996) *J. Biol. Chem.* **271,** 11376–11382
57. Mohler, K. M., Sleath, P. R., Fitzner, J. N., Cerretti, D. P., Alderson, M., Kerwar, S. S., Torrance, D. S., Otten-Evans, C., Greenstreet, T., Weerawarna, K., Kronheim, S. R., Petersen, M., Gerhart, M., Kozlosky, C. J., March, C. J., and Black, R. A. (1994) *Nature* **370,** 218–220
58. Crowe, P. D., Walter, B. N., Mohler, K. M., Otten-Evans, C., Black, R. A., and Ware, C. F. (1995) *J. Exp. Med.* **181,** 1205–1210
59. Tsubuki, S., Saito, Y., Tomioka, M., Ito, H., and Kawashima, S. (1996) *J Biochem.* (*Tokyo*) **119,** 572–576
60. Figueiredo-Pereira, M. E., Berg, K. A., and Wilk, S. (1994) *J. Neurochem.* **63,** 1578–1581
61. Coux, O., Tanaka, K., and Goldberg, A. L. (1996) *Annu. Rev. Biochem.* **65,** 801–847
62. Fenteany, G., Standaert, R. F., Lane, W. S., Choi, S., Corey, E. J., and Schreiber, S. L. (1995) *Science* **268,** 726–731
63. Tanaka, K. (1995) *Mol. Biol. Rep.* **21,** 21–26
64. Hung, A. Y., Haass, C., Nitsch, R. M., Qiu, W. Q., Citron, M., Wurtman, R. J., Growdon, J. H., and Selkoe, D. J. (1993) *J. Biol. Chem.* **268,** 22959–22962
65. Dyrks, T., Monning, U., Beyreuther, K., and Turner, J. (1994) *FEBS Lett.* **349,** 210–214
66. Elbein, A. D. (1987) *Methods Enzymol.* **138,** 661–709
67. Dovey, H. F., John, V., Anderson, J. P., Chen, L. Z., de Saint Andrieu, P., Fang, L. Y., Freedman, S. B., Folmer, B., Goldbach, E., Holsztynska, E. J., Hu, K. L., Johnson-Wood, K. L., Kennedy, S. L., Kholodenko, D., Knops, J. E., Latimer, L. H., Lee, M., Liao, Z., Lieberburg, I. M., Motter, R. N., Mutter, L. C., Nietz, J., Quinn, K. P., Sacchi, K. L., Seubert, P. A., Shopp, G. M., Thorsett, E. D., Tung, J. S., Wu, J., Yang, S., Yin, C. T., Schenk, D. B., May, P. C., Altstiel, L. D., Bender, M. H., Boggs, L. N., Britton, T. C., Clemens, J. C., Czilli, D. L., Dieckman-McGinty, D. K., Droste, J. J., Fuson, K. S., Gitter, B. D., Hyslop, P. A., Johnstone, E. M., Li, W. Y., Little, S. P., Mabry, T. E., Miller, F. D., and Audia, J. E. (2001) *J. Neurochem.* **76,** 173–181
68. Zhong, Z., Higaki, J., Murakami, K., Wang, Y., Catalano, R., Quon, D., and Cordell, B. (1994) *J. Biol. Chem.* **269,** 627–632
69. Sisodia, S. S., Koo, E. H., Beyreuther, K., Unterbeck, A., and Price, D. L. (1990) *Science* **248,** 492–495
70. Sahasrabudhe, S. R., Spruyt, M. A., Muenkel, H. A., Blume, A. J., Vitek, M. P., and Jacobsen, J. S. (1992) *J. Biol. Chem.* **267,** 25602–25608
71. Maruyama, K., Kametani, F., Usami, M., Yamao-Harigaya, W., and Tanaka, K. (1991) *Biochem. Biophys. Res. Commun.* **179,** 1670–1676
72. Parvathy, S., Hussain, I., Karran, E. H., Turner, A. J., and Hooper, N. M. (1998) *Biochem. Soc. Trans.* **26,** 242
73. Turner, R. T., III, Koelsch, G., Hong, L., Castanheira, P., Ermolieff, J., Ghosh, A. K., Tang, J., Castenheira, P., and Ghosh, A. (2001) *Biochemistry* **40,** 10001–10006
74. Citron, M., Teplow, D. B., and Selkoe, D. J. (1995) *Neuron* **14,** 661–670
75. Kitazume, S., Tachida, Y., Oka, R., Shirotani, K., Saido, T. C., and Hashimoto, Y. (2001) *Proc. Natl. Acad. Sci. U. S. A.* **98,** 13554–13559
76. Kitazume, S., Tachida, Y., Oka, R., Kotani, N., Ogawa, K., Suzuki, M., Dohmae, N., Takio, K., Saido, T. C., and Hashimoto, Y. (2003) *J. Biol. Chem.* **278,** 14865–14871
77. Lichtenthaler, S. F., Dominguez, D. I., Westmeyer, G. G., Reiss, K., Haass, C., Saftig, P., De Strooper, B., and Seed, B. (2003) *J. Biol. Chem.* **278,** 48713–48719
78. Haass, C., Schlossmacher, M. G., Hung, A. Y., Vigo-Pelfrey, C., Mellon, A., Ostaszewski, B. L., Lieberburg, I., Koo, E. H., Schenk, D., Teplow, D. B., and Selkoe, D. J. (1992) *Nature* **359,** 322–325
79. Lichtenthaler, S. F., Wang, R., Grimm, H., Uljon, S. N., Masters, C. L., and Beyreuther, K. (1999) *Proc. Natl. Acad. Sci. U. S. A.* **96,** 3053–3058
80. Lichtenthaler, S. F., Beher, D., Grimm, H. S., Wang, R., Shearman, M. S., Masters, C. L., and Beyreuther, K. (2002) *Proc. Natl. Acad. Sci. U. S. A.* **99,** 1365–1370
81. Murphy, M. P., Hickman, L. J., Eckman, C. B., Uljon, S. N., Wang, R., and Golde, T. E. (1999) *J. Biol. Chem.* **274,** 11914–11923
82. Tischer, E., and Cordell, B. (1996) *J. Biol. Chem.* **271,** 21914–21919
83. Zhang, J., Ye, W., Wang, R., Wolfe, M. S., Greenberg, B. D., and Selkoe, D. J. (2002) *J. Biol. Chem.* **277,** 15069–15075
84. Weihofen, A., Binns, K., Lemberg, M. K., Ashman, K., and Martoglio, B. (2002) *Science* **296,** 2215–2218
85. Brown, M. S., Ye, J., Rawson, R. B., and Goldstein, J. L. (2000) *Cell* **100,** 391–398
86. Lee, J. R., Urban, S., Garvey, C. F., and Freeman, M. (2001) *Cell* **107,** 161–171
87. Urban, S., Lee, J. R., and Freeman, M. (2002) *EMBO J.* **21,** 4277–4286
88. Sato, T., Dohmae, N., Qi, Y., Kakuda, N., Misonou, H., Mitsumori, R., Maruyama, H., Koo, E. H., Haass, C., Takio, K., Morishima-Kawashima, M., Ishiura, S., and Ihara, Y. (2003) *J. Biol. Chem.* **278,** 24294–24301
89. Scheinfeld, M. H., Ghersi, E., Laky, K., Fowlkes, B. J., and D'Adamio, L. (2002) *J. Biol. Chem.* **277,** 44195–44201
90. May, P., Bock, H. H., Nimpf, J., and Herz, J. (2003) *J. Biol. Chem.* **277,** 18736–18743